

Reconstruction of a system's dynamics from short trajectories

C. Komalapriya,^{1,*} M. Thiel,² M. C. Romano,^{2,3} N. Marwan,^{1,5} U. Schwarz,¹ and J. Kurths^{1,4,5}

¹*Center for Dynamics of Complex Systems, University of Potsdam, 14415 Potsdam, Germany*

²*Department of Physics, University of Aberdeen, Aberdeen AB24 3UE, United Kingdom*

³*Institute of Medical Sciences, University of Aberdeen, Aberdeen AB25 2ZD, United Kingdom*

⁴*Department of Physics, Humboldt University Berlin, 12489 Berlin, Germany*

⁵*Potsdam Institute for Climate Impact Research, 14412 Potsdam, Germany*

(Received 3 March 2008; revised manuscript received 2 September 2008; published 24 December 2008)

Long data sets are one of the prime requirements of time series analysis techniques to unravel the dynamics of an underlying system. However, acquiring long data sets is often not possible. In this paper, we address the question of whether it is still possible to understand the complete dynamics of a system if only short (but many) time series are observed. The key idea is to generate a single long time series from these short segments using the concept of recurrences in phase space. This long time series is constructed so as to exhibit a dynamics similar to that of a long time series obtained from the corresponding underlying system.

DOI: [10.1103/PhysRevE.78.066217](https://doi.org/10.1103/PhysRevE.78.066217)

PACS number(s): 05.45.Tp, 05.45.Pq

I. INTRODUCTION

The analysis of the dynamics of a system from measured data usually requires rather long time series. Practically, acquiring long time series from natural systems is feasible only in some cases and is often impossible in many due to experimental restrictions. In some cases, the costs involved in a particular experiment might make the acquisition of such long time series very difficult. In other cases, it might be the nature of the system itself, which does not allow recording long time series. Typical examples of the latter case include earthquake data, seizure data, financial records, and paleoclimatological data. The problem of short data sets also prevails among the modeling community. For example, modeling of systems such as atmosphere or protein molecules involves numerous system parameters and variables. Simulating such high dimensional systems for studying their long term dynamics is a tedious task and is also restricted on the computational front. However, understanding the dynamics of the above mentioned systems is crucial for the corresponding fields of research.

Several methods of time series analysis, such as wavelets or recurrence plots [1], have been applied to analyze short data sets. However, there are still many open problems and questions, e.g., how short is too short for a given time series analysis method? In this paper we approach the problem differently. We propose an algorithm which reconstructs the dynamics of an unknown system observed at many different instances but for a short period of time only. The key idea, which allows us to tackle the problem, is that even short segments of a time series contain some (local) information about the flow. We use this information, i.e., the short trajectories themselves, as building blocks to reconstruct rather long trajectories, which we call dynamically reconstructed trajectories (DRTs). The DRTs closely resemble the dynamics of the underlying system and can then be treated like any other long trajectory (LT), so that any standard data analysis methods can be applied to investigate them.

The algorithm that we propose to generate DRTs is based on the concept of recurrences [2], which is in turn linked to the well-known ergodic theory. The phase space trajectories of measure preserving dynamical systems come back in close proximity to any former phase space point after a sufficiently long time, due to their ergodic nature. It is this “recurrence” property of dynamical systems that we utilise in our algorithm. The concept of recurrences has already been used to understand different aspects of the dynamics of a wide range of model and real world systems. A related method called recurrence plots (RPs) [3] has been shown to be useful for the detection of transitions in the dynamics of complex systems [4–7], synchronization analysis and detection of nonlinear correlations [8], estimation of system invariants [9], and even generation of surrogates [10,11]. Furthermore, RPs have found applications in numerous fields of research such as life sciences [12], engineering [13,14], earth sciences [15–17], and astrophysics [18–20]. A method related to our approach has been proposed to deal with the problems related to transient chaos [21].

The organization of the paper is as follows. In Sec. II we propose an algorithm that generates DRTs. We compare the generated DRTs to LTs in terms of linear and nonlinear measures, which are described in Sec. III. We then apply the proposed algorithm to paradigmatic dynamical systems in Sec. IV. In Secs. V and VI we study the robustness of our approach with respect to the choice of the parameters of the algorithm and the number and length of the given short trajectories. In Sec. VII we show how to reconstruct a DRT from trajectories consisting of only two points and in Sec. VIII we discuss the application of the algorithm to an ensemble of scalar time series. We study the effect of noise on the algorithm in Sec. IX. Finally we apply the algorithm to real world data sets from electrochemical oscillators in Sec. X before concluding in Sec. XI.

II. ALGORITHM

Suppose that we have obtained a set of K short trajectories each of length N , i.e., $\vec{x}_1^1, \dots, \vec{x}_N^1; \vec{x}_1^2, \dots, \vec{x}_N^2; \dots; \vec{x}_1^K, \dots, \vec{x}_N^K$

*komala@agnld.uni-potsdam.de

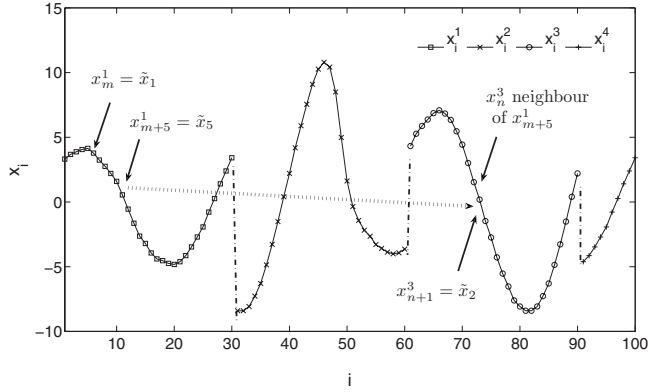


FIG. 1. Algorithm to construct DRTs from short trajectories. The short trajectories which are concatenated are marked with different symbols. The data points $\tilde{x}_1, \tilde{x}_2, \dots, \tilde{x}_{L_D}$ denote the generated DRT. For a detailed explanation of the procedure, see Sec. II.

from a series of measurements and simulations. The vector $\vec{x}_i^j \in \mathcal{R}^d$ denotes the phase space vector at time i of the trajectory j in a d -dimensional phase space. Assuming that the system under investigation is ergodic, the ensemble of short trajectories started at many different random times or that have been successively measured at different stages of a single experiment will contain all the important (local) information about the dynamics. A dynamically reconstructed trajectory is then generated by the following algorithm (see Fig. 1).

(1) First, the short trajectories are appended to generate one long concatenated trajectory $\vec{x}_1, \dots, \vec{x}_L$ where $L=NK$.

(2) We compute the set of neighbors of each phase space vector \vec{x}_i of the concatenated trajectory with respect to a threshold ξ , i.e., we determine the set $\mathcal{N}_i = \{\vec{x}_j \mid \|\vec{x}_i - \vec{x}_j\| < \xi\}$ for $i=1, \dots, L$, where $\|\cdot\|$ is a norm, e.g., the Euclidean or the Maximum norm.

(3) A point \vec{x}_m is then randomly chosen from the concatenated trajectory, where $m < L$. This point is the first one of the DRT.

(4) Next, we distinguish between the following two situations. (i) If \vec{x}_m is not at the end of a short segment, i.e., if $m \bmod N \neq 0$, we jump to the future [22] of one of the neighbors of \vec{x}_m with probability p . That means, we generate a random number r between 0 and 1; if $r < p$, we choose randomly between one of the neighbors [23] of \vec{x}_m and take its future as the next point of our DRT. Otherwise, i.e., if $r > p$, we choose \vec{x}_{m+1} as the next point of the DRT. (ii) If \vec{x}_m is at the end of a short segment, i.e., if $m \bmod N = 0$, we jump to the future of one of its neighbors, since \vec{x}_m has not a “proper” future.

(5) The above steps are repeated until a DRT of length L_D is generated, where L_D is the desired length for the DRT and fulfills $L_D \leq L$.

During the DRT generation, it is, in principle, possible that we arrive at a point \vec{x}_i , which is at the end of a short segment but has no neighbors with respect to ξ , except for itself. In this case, we run the algorithm again but starting at a different initial point \vec{x}_m . If the number of trials T to generate a DRT exceeds a certain threshold, e.g., $T > 1000$, the process is aborted assuming that it is not possible to find a

DRT for the given ensemble of short trajectories and chosen set of parameters ξ and p of the algorithm. This, however, does not mean that the algorithm fails. It is just an indication that the parameters ξ and p have not been chosen appropriately.

In the next sections, we show that the DRTs reproduce very well the dynamics of the underlying system. For this purpose, we compare an ensemble of original LTs to an ensemble of DRTs with respect to linear and nonlinear measures that characterize the dynamics.

III. ASSESSMENT OF THE QUALITY OF THE DRTs

To demonstrate that DRTs can reproduce the dynamics of the underlying system, we compare the generated DRTs to the original long trajectories (LTs) with respect to the following measures: (i) the correlation time τ_c of the autocorrelation function $C(\tau)$ [24], (ii) the first minimum τ_m of the mutual information function $M(\tau)$ [24], and (iii) the mean diagonal line length \bar{D} of the recurrence plot of the trajectory, which is an estimate for the Rényi Entropy of second order (K_2) (Appendix).

The correlation time τ_c is a linear measure for the time during which points of the time series are correlated. The first minimum τ_m of the mutual information is a nonlinear measure for the time during which points of the time series contain information about each other. The mean diagonal line length \bar{D} is estimated from the recurrence plot and it characterizes the predictability of a given system. There are two main reasons to choose \bar{D} for assessing the quality of the generated DRTs: (i) it is closely related to K_2 [1] which is a dynamical invariant measure (not a topological one) of a given system and (ii) is computationally faster to determine than K_2 . In Sec. IV we provide the estimates of both \bar{D} and of K_2 to demonstrate the potential our algorithm. In the later sections, where we investigate the robustness of our algorithm with respect to different parameters and the effects of noise, we estimate only \bar{D} because of computational efficiency.

IV. CASE STUDIES

We test the validity of our algorithm by applying it to three paradigmatic chaotic systems: the Bernoulli shift map, the Hénon map, and the Rössler oscillator. For these three cases, we numerically simulate the dynamical equations of the respective systems to generate K short trajectories, each of length N . Then we construct DRTs using the proposed algorithm. We first exemplify the results for a specific set of parameters ξ and p . We show that in all three cases the proposed algorithm successfully generates DRTs that mimic the properties of a LT of the respective system. In Sec. V we will study how the results depend on the specific choice of the parameters ξ and p . Also we will investigate the robustness of the algorithm with respect to the length N and number K of short trajectories.

A. Bernoulli map

First, we consider the Bernoulli map

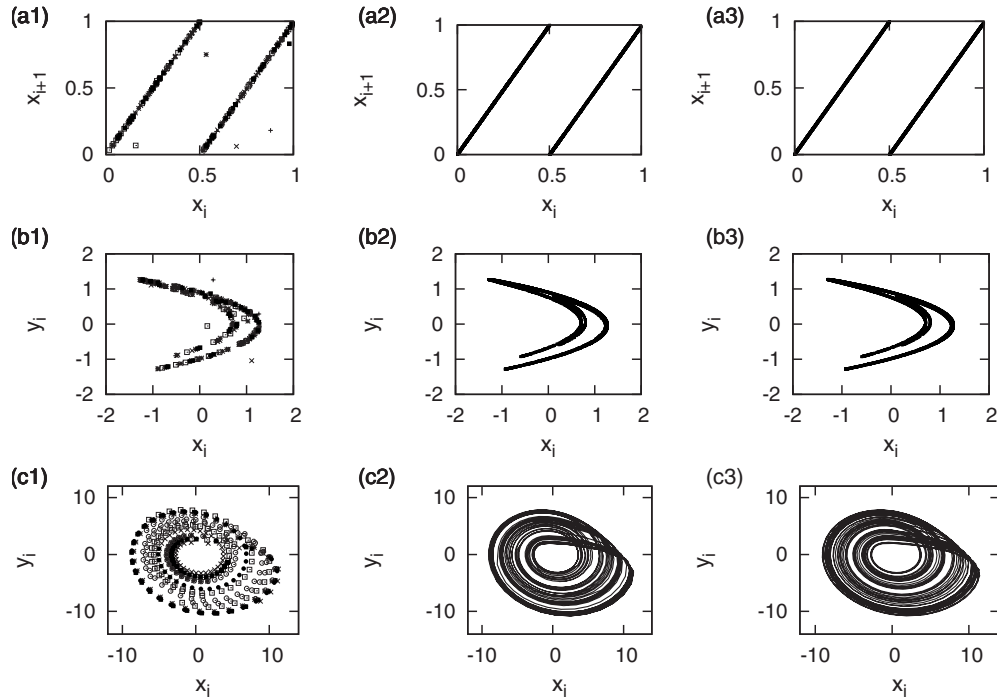


FIG. 2. Phase portraits before (a1, b1, and c1) and after (a2, b2, and c2) applying the reconstruction algorithm for (a) the Bernoulli map, (b) the Hénon map, and (c) the Rössler oscillator. Phase portraits of the three systems obtained from their respective LTs are given in a3, b3, and c3 for comparison. Note that in a1, b1, and c1 the different short trajectories of the ensemble are plotted with different point types.

$$x_{i+1} = 2x_i \text{ mod } 1. \tag{1}$$

Starting at 100 different initial conditions, Eq. (1) is iterated to generate short trajectories of length 40, i.e., $N=40$ and $K=100$. The generated short trajectories are appended to generate a concatenated trajectory of length $L=4000$. Figure 2(a1) shows the return map of the concatenated trajectory, where the “jumps” or discontinuities between the short segments are clearly seen. It is clear that the last point of a short segment is independent of the first point of the next short segment. Therefore, at these points, $x_{i+1} \neq 2x_i \text{ mod } 1$. Then, the set of neighbors \mathcal{N}_i of each data point is estimated for a threshold $\xi=0.001$. Setting $p=0.03$ and following the steps of the algorithm, we generate a DRT of length $L_D=4000$. The phase portrait of the generated DRT is shown in Fig. 2(a2). Note that it perfectly reproduces the phase portrait of a LT [Fig. 2(a3)].

Moreover, we compute the autocorrelation function and the mutual information for the generated DRT and for a LT [Figs. 3(a1) and (a2); DRT (solid line), LT (dashed line)]. It is clearly seen that up to statistical fluctuations, the DRT reproduces both, the autocorrelation function and the mutual information, very well. The autocorrelation function of both DRT and LT decays to the critical value of $1/e$ at $\tau_c=2$. Analogously, the mutual information of both DRT and LT has its first minimum at $\tau_m=4$. The mean diagonal line length \bar{D} estimated from the RP of the DRT is 2.02 and that of the LT is 2.00. Both values are very close to the expected analytical value of 2.0. Moreover, the estimated value of K_2 from the DRT is 0.69 ± 0.00 , while the same estimated from the LT is 0.69 ± 0.00 . Both of them are in agreement with the theoretical value of $\ln(2)$.

B. Hénon map

Next, we analyze the Hénon map [25]

$$x_{i+1} = 1 - ax_i^2 + by_i,$$

$$y_{i+1} = x_i \tag{2}$$

in the chaotic regime ($a=1.4$ and $b=0.3$). Starting at different initial conditions, Eqs. (2) are iterated to generate 100

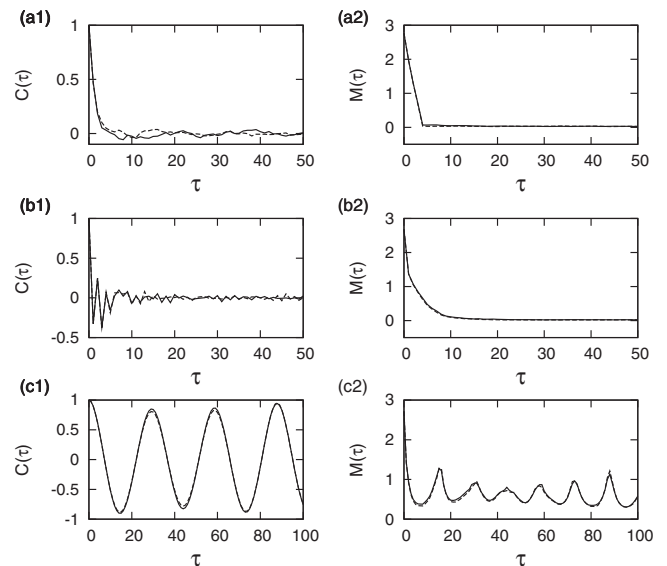


FIG. 3. Autocorrelation function (a1, b1, and c1) and mutual information (a2, b2, and c2) of a DRT (solid line) and a LT (dashed line) plotted in dependence of the lag τ . (a) Bernoulli map, (b) Hénon map, and (c) Rössler oscillator.

short trajectories of length 60 each, i.e., $N=60$ and $K=100$. The generated short trajectories are appended to generate a concatenated trajectory. Figure 2(b1) shows the phase portrait of the concatenated trajectory, where the discontinuities between the short segments are clearly seen. Following the procedure described in Sec. II, a two-dimensional DRT of length $L_D=6,000$ is generated with parameters $\xi=0.01$ and $p=0.03$.

Again the phase portrait of the DRT reproduces very well that of the original Hénon map [Figs. 2(b2) and 2(b3)]. The autocorrelation function and mutual information estimated from the x component of the reconstructed trajectory also reproduce well the corresponding functions of the original system [Figs. 3(b1) and 3(b2)]. The correlation time for both DRT and LT is $\tau_c=1$ and the mutual information reaches its minimal value at $\tau_m=10$ for both DRT and LT. The mean diagonal line length \bar{D} of the recurrence plot of the DRT and that of the LT is 2.47 and 2.44, respectively. Both of them are well in agreement with the expected value 2.474 [26]. The estimated K_2 of the DRT is 0.33 ± 0.01 and differs slightly from that computed from a LT, 0.32 ± 0.02 . Again both values are close to the expected value of 0.32 [27].

C. Rössler oscillator

Finally, we apply the reconstruction algorithm to an ensemble of short trajectories from the Rössler oscillator in a chaotic regime [28]

$$\begin{aligned}\dot{x} &= -y - z, \\ \dot{y} &= x + ay, \\ \dot{z} &= b + (x - c)z,\end{aligned}\quad (3)$$

with the parameters $a=b=0.2$ and $c=5.7$. We generate short trajectories starting at different initial conditions using the fourth order Runge-Kutta algorithm. The integration step is $h=0.01$ and we sample every 20th point, i.e., the sampling time is 0.2. We generate 500 trajectories, each of length $N=50$ (corresponding to about 1.5 oscillations only). In this case, we fix the parameters as follows: $\xi=0.1$ and $p=0.03$. We then generate a three-dimensional DRT of length $L_D=5000$.

The generated DRT is found to have a smooth attractor that reproduces the phase portrait of the chaotic Rössler oscillator rather well [Figs. 2(c2) and 2(c3)]. The autocorrelation function of both DRT and LT reaches the critical value of $1/e$ at a lag of $\tau_c=7$ [Fig. 3(c1)] and the mutual information has its minimum at $\tau_m=8$ for both DRT and LT [Fig. 3(c2)]. In fact, the autocorrelation function and the mutual information of the DRT and LT coincide almost perfectly. Moreover, the mean diagonal line \bar{D} for the DRT is 10.21 and that for the LT is 10.25.

Due to the nonhyperbolicity of the Rössler attractor, there exist two time scales and hence two different K_2 values [9]. While the first K_2 value characterises the short term dynamics and amplitude fluctuations of the system (K_2^S), the second scaling region corresponds to the long term dynamics and

phase diffusion of the attractor (K_2^L). However, both K_2 estimates are important as they measure predictability of a single attractor on two different time scales.

The K_2 estimates of the DRT generated are as follows: (i) $K_2^S=0.23 \pm 0.00$ and (ii) $K_2^L=0.10 \pm 0.02$. The corresponding values estimated from a LT are 0.23 ± 0.04 and 0.07 ± 0.04 . The K_2^S estimates of both the DRT and LT are rather close to the literature value of 0.23 [9]. However, the K_2^L of the DRTS deviates from the expected value of 0.07 [9] due to the frequent jumps made by the algorithm during the reconstruction process. However, results suggest that a better value of K_2^L can be obtained if the jumps induced by the algorithm are limited by either increasing N or decreasing p .

We have shown the potential of our method by applying it to three different prototypical chaotic systems. In the next section we systematically analyse the robustness of our algorithm with respect to the choice of the two parameters of the algorithm. Furthermore, we study the performance of the algorithm by varying the length and number of short trajectories.

V. ROBUSTNESS OF THE ALGORITHM

The quality of a DRT using the proposed method depends on the length N and the number K of short trajectories, as well as on the choice of the threshold ξ and the value of p . In order to quantify how well the generated DRTs reproduce the dynamics of the underlying system depending on these parameters, we apply the following procedure.

We generate K short trajectories of N points each. We append them and from this concatenated trajectory, we generate an ensemble of 100 different DRTs of length L_D , by choosing different starting points randomly.

We generate an ensemble of 100 LTs from the original system, each of length L_D .

To quantify how close both ensembles are, we compute the following errors with respect to the three different statistics introduced in Sec. III. We compare the autocorrelation function and the mutual information of the two different ensembles for $1 \leq \tau \leq \tau_{\max}$. The error for the autocorrelation function and the mutual information, respectively, is estimated as follows:

$$E_{CM} = \frac{1}{\tau_{\max}} \sum_{\tau=1}^{\tau_{\max}} \frac{|\mu(\tau) - \mu'(\tau)|}{0.5[\sigma(\tau) + \sigma'(\tau)]}, \quad (4)$$

where $\mu(\tau)$ is the mean value of the autocorrelation function at lag τ of the ensemble of DRTs, and $\mu'(\tau)$ is the mean value of the autocorrelation function at lag τ of the ensemble of LTs. Similarly, $\sigma(\tau)$ and $\sigma'(\tau)$ are the standard deviations of the autocorrelation function at lag τ estimated from 100 realisations of DRTs and LTs, respectively. The error for the mutual information function (E_M) is computed analogously. In the case of the \bar{D} , we estimate the error simply as

$$E_{\bar{D}} = \frac{|\mu - \mu'|}{0.5(\sigma + \sigma')}, \quad (5)$$

where μ and μ' represent the average \bar{D} over 100 DRTs and 100 LTs, respectively, and σ and σ' are the estimated stan-

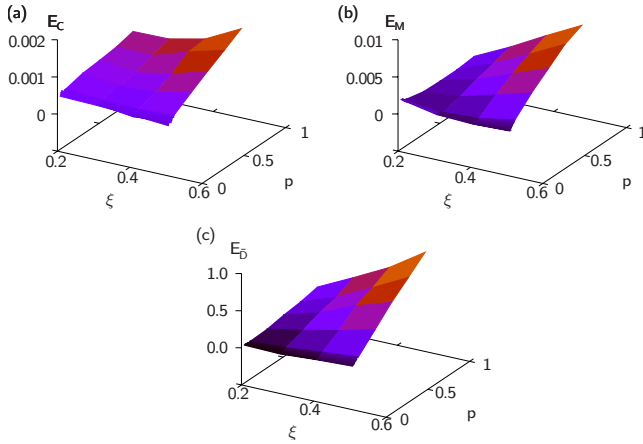


FIG. 4. (Color online) Errors in dependence of the probability p to jump and on the threshold ξ for the Rössler system. Error in (a) the autocorrelation function, (b) the mutual information, and (c) the mean diagonal line.

dard deviations. That means, $E_{\bar{D}} \sim 1$ if the difference between the expected values is of the same size as the standard deviation of both ensembles (LTs and DRTs); in contrast, $E_{\bar{D}} \ll 1$ indicates a very small difference between both expected values. The same holds for $E_{C/M}$.

Now we present the results of the sensitivity studies carried out with respect to each of the parameters ξ and p , as well as the given number K of the short trajectories and their length N . We exemplify the results obtained for the Rössler system, since the results for the Bernoulli and the Hénon map are qualitatively the same.

A. Sensitivity with respect to p and ξ

To investigate the influence of the values of p and ξ in the generation of DRTs, we first fix $N=50$ and $K=1000$, and vary p and ξ systematically. For each set of values of p and ξ , we generate 100 DRTs of length $L_D=5000$ and compare them to 100 LTs from the underlying system.

In Fig. 4 we show the errors in the autocorrelation function (a), mutual information (b), and mean diagonal line (c) for the Rössler system in dependence of the probability p to jump and on the threshold ξ . For all three measures, the error increases with p , as expected. This is because if p increases, we jump more frequently to the future of the neighbors instead of staying on the same short trajectory. Due to these frequent jumps, the errors accumulate and we see a deviation of the ensemble of DRTs from the ensemble of LTs with respect to the considered measures. However, it is remarkable that even for $p=1.0$, i.e., if we allow the trajectory to jump at every point, the errors are rather small. For example, the maximal error in the mutual information is 1% [Fig. 4(b)]. Furthermore, if $p > 0.1$ the errors also increase with the threshold ξ . This is due to the fact that a large threshold will lead to larger jumps, and therefore the errors will become larger.

A blow-up of the errors for $p < 0.1$ reveals that there is a minimum in the error for intermediate values of ξ , namely, at about $\xi=0.35$ [most clearly seen in Fig. 5(b)]. This is due to

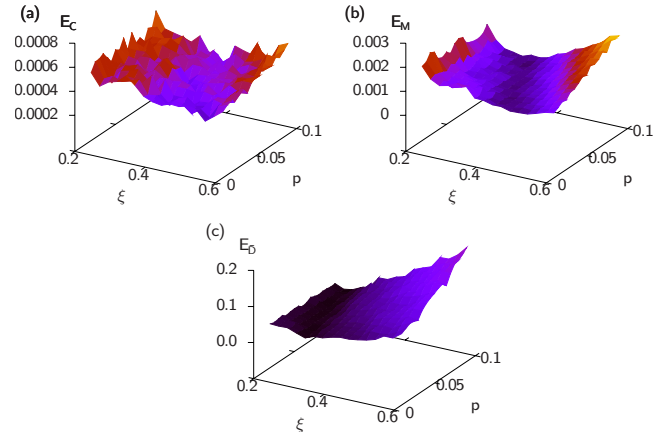


FIG. 5. (Color online) Zoom of the errors for small values of p and in dependence of the threshold ξ for the Rössler system. Error in (a) the autocorrelation function, (b) the mutual information, and (c) the mean diagonal line.

the fact that for very small values of p , we practically jump only at the end of a short segment. Hence, if the threshold ξ is too small, then the number of neighbors of the points at the end of the short segments will be very low. This decreases the number of possible points to which we can jump, leading to a repetition of the segments used in the reconstructed trajectory. Hence, the algorithm generates a DRT which is more predictable than the LTs. For this reason, if p is small, it is better to use a larger threshold ξ than the threshold that we would choose for larger values of p .

Summarizing, Figs. 4 and 5 clearly show that good DRTs can be generated for appropriate values of p and ξ . The magnitude of the errors is the smallest for the autocorrelation function and the highest for the mean diagonal line length. Nevertheless, even for \bar{D} , the maximal error is less than one standard deviation of the distribution \bar{D} of LTs. Hence, we can conclude that, either if we stay on a short trajectory as long as possible and choose an intermediate value for the threshold ξ , or if we stay just a few steps on a short trajectory and use a very small value of ξ , we can reproduce the underlying dynamics rather closely.

B. Sensitivity with respect to N and K

It is also important to investigate the influence of the length N and the number K of short trajectories on the quality of the generated DRTs. In practice, these values are fixed by the given experimental conditions. Therefore, it is crucial to study the dependence of the results on these values to explore the limits of the applicability of the proposed algorithm. We fix the values of the parameters to $\xi=0.3$ and $p=0.05$ and vary N and K systematically.

The error estimates for the autocorrelation function, the mutual information and the mean diagonal line calculated for the Rössler system are shown in Figs. 6(a)–6(c), respectively. For small values of N and K , the errors increase abruptly for all of the three measures. However, when N and K are sufficiently large, the difference between the generated DRTs and the LTs is rather small. Again, the error in the

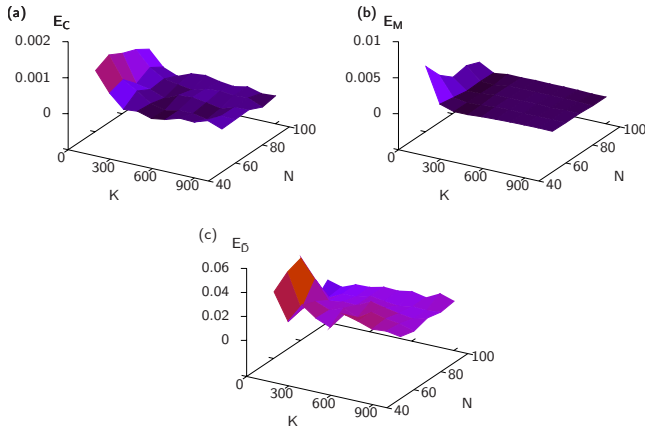


FIG. 6. (Color online) Errors in dependence of the length N and the number K of short trajectories for the Rössler oscillator with respect to (a) the autocorrelation function, (b) the mutual information function, and (c) the mean diagonal line.

autocorrelation is one and two orders of magnitude smaller than the error in the mutual information and mean diagonal line, respectively. But remarkably, note that even in the worst case, i.e., for low values of N and K , the errors are still very small. Therefore, even for a rather low number of very short trajectories, it is possible to reconstruct the underlying dynamics to a rather good extent.

VI. AVERAGE NUMBER OF CONSECUTIVE STEPS ON ONE SHORT TRAJECTORY

In this section we calculate analytically the average number of consecutive time steps $\langle n \rangle$ spent on a single short trajectory before jumping to another short trajectory. This average number of steps is determined by two parameters. The length N of the short trajectories, since once we have reached the end of a short trajectory, we necessarily have to jump to the future of one of the neighbors of the last point of the short trajectory and the probability p to jump to the future of a neighbor.

It can be shown, that the average number of consecutive steps on a certain short trajectory is given by

$$\begin{aligned} \langle n \rangle &= \frac{1}{N-1} \sum_{k=1}^{N-1} \left\{ (1-p)^k k + \sum_{i=1}^{k-1} ip(1-p)^i \right\} \\ &= \frac{1-p}{N-1} \left\{ \frac{(1-p)^N}{p^2} + \frac{N}{p} - \frac{1}{p^2} \right\}. \end{aligned} \quad (6)$$

From Eq. (6) we can distinguish the following cases.

(1) If $p=0$ and $N \rightarrow \infty$, then $\langle n \rangle \rightarrow \infty$. This corresponds to not allowing the trajectory to jump before it reaches the end of a short trajectory. Then, the DRT algorithm only jumps at the end of a segment, but since $N \rightarrow \infty$, obviously also $\langle n \rangle \rightarrow \infty$.

(2) If $p=1$ and $N \rightarrow \infty$, then $\langle n \rangle = 0$. This corresponds to the case that the DRT algorithm jumps to the future of one of its neighbors at every point. Therefore, the average number of consecutive steps on a short trajectory is zero.

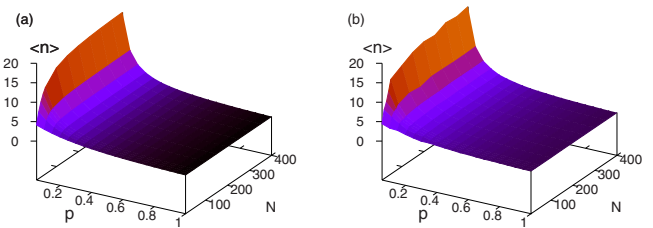


FIG. 7. (Color online) Average number of consecutive steps $\langle n \rangle$ on a short trajectory in dependence of N and p . (a) Theoretical value of $\langle n \rangle$ given by Eq. (6). (b) $\langle n \rangle$ computed numerically for the Rössler oscillator for $K=5000$ trajectories.

(3) If $0 < p < 1$ and $N \rightarrow \infty$, then $\langle n \rangle = (1-p)/p$. In this case we do not have the finite size effect due to the short trajectories, and hence, have a geometric distribution.

The average number of consecutive steps $\langle n \rangle$ analytically estimated by Eq. (6) is compared to that obtained from the numerical simulations in Fig. 7. The analytical and the numerical results coincide almost perfectly.

Since we know the dependence of the number $\langle n \rangle$ on N and p , we can argue how the error of the generated DRTs with respect to LTs depends on $\langle n \rangle$. In order to do this, we compute the error in the mutual information in dependence of N and p for $K=5000$ short trajectories of the Rössler system and a threshold $\xi=0.03$ (Fig. 8). We observe that for $p > 0.05$, irrespective of the value that N takes, the error in the mutual information monotonously increases with p [Fig. 8(a)]. This is in accordance with Fig. 7, where we see that for $p > 0.05$, the value of consecutive number of steps on one trajectory is almost independent of N . High values of p imply frequent jumps and therefore, a small average number of steps $\langle n \rangle$ on a short trajectory and also an accumulation of errors.

On the other hand, for small values of p ($0 < p < 0.05$), the average number of steps $\langle n \rangle$ is also strongly affected by N (Fig. 7). If p is small, then too large values of N would lead to a situation where we repeat short segments, because we do not have enough possibilities to jump to neighbors (only at the end of the segments). Therefore, for small values of p , the error between DRTs and LTs will be minimal at intermediate values of N . This is observed in Fig. 8(a), where we find a minimum in the error with respect to the mutual information for $N \approx 50$.

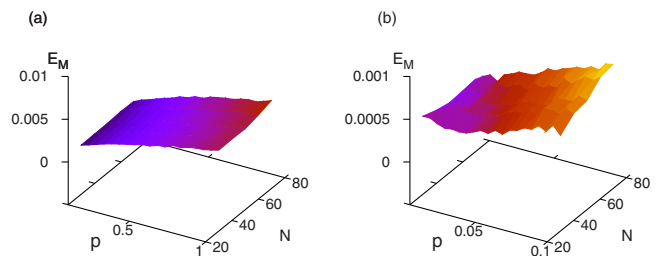


FIG. 8. (Color online) Error with respect to the mutual information for the Rössler oscillator in dependence of N and p , or implicitly, the average number $\langle n \rangle$ of consecutive steps on a short trajectory. (a) Whole region of p , (b) zoom for small values of p .

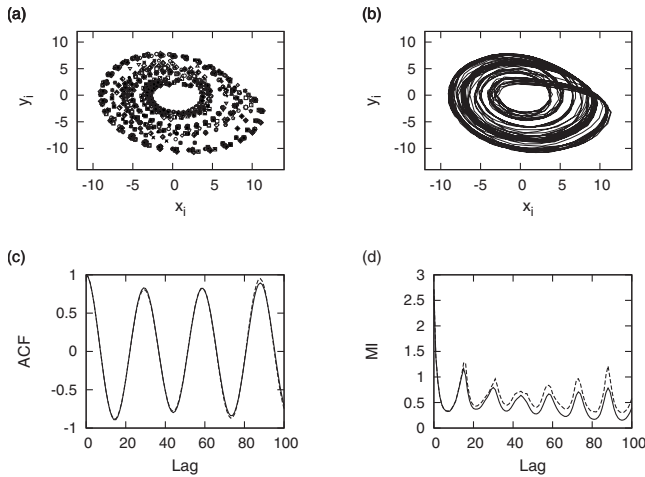


FIG. 9. Application of the reconstruction algorithm to short trajectories consisting of only two consecutive phase space points from the Rössler system. (a) Phase space projection of the long concatenated trajectory, which is the start for the reconstruction algorithm. Here again, the different short trajectories of the ensemble are plotted with different point types. (b) Phase space projection of the DRT. (c) The autocorrelation function of the DRT (solid line) and that of an original LT (dashed line). (d) The mutual information function of the DRT (solid line) and that of an original LT (dashed line).

VII. RECONSTRUCTION FROM TWO-POINT TRAJECTORIES

In the preceding sections, we have compared the generated DRTs to original LTs with respect to linear and nonlinear measures. We assessed the quality of the DRTs in dependence of the parameters ξ and p of the reconstruction algorithm and the number K of available short trajectories and their length N . We have seen that the largest errors are made for large values of p . On the other hand, note that N and p are related, e.g., $p=1$ is equivalent to have short trajectories consisting of only two consecutive points, i.e., $N=2$. Note also that the largest errors committed in these cases are still very small, namely, less than one standard deviation of the corresponding distribution (Figs. 4 and 8). Therefore, we have shown that even in this extreme case, where we have very little local information about the flow, one can still recover most of the information of the underlying dynamics.

In order to illustrate this extreme case, we generate a DRT of the Rössler oscillator from an ensemble of short trajectories ($K=30\,000$) consisting of just two phase points ($N=2$), for the parameters $p=1.0$ and $\xi=0.3$. The phase portrait of the concatenated trajectory and the phase portrait of the generated DRT are shown in Figs. 9(a) and 9(b), respectively.

We observe that the state space projection of the DRT closely reproduces the phase space projection of the original Rössler system [Fig. 2(c2)]. Furthermore, the autocorrelation function of the DRT is almost identical to that of the original LT [Fig. 9(c)]. Hence, we can state that the reconstruction algorithm generates DRTs which reproduce the dynamics of the underlying systems rather well, even from short trajectories consisting of just two consecutive phase space points.

It is important to mention here that even if we have two consecutive points in the phase space, the number of short

trajectories must be large enough, to cover the entire attractor, and the distance between the consecutive phase space points must be small enough to obtain the relevant information about the local flow. If any of these conditions is not fulfilled, then a more conservative estimation of the required length of the univariate segments is given by the longest characteristic time scale of the underlying system.

Note that the reconstruction from an ensemble of scalar time series consisting of two points would not be possible. This is because in this case, we have to first embed each short univariate time series (see Sec. VIII). For this we would need an ensemble of time series of length $N \geq 2 + (m-1)\tau$ (where m is the embedding dimension and τ the embedding delay) in order to get two-point trajectories in phase space.

VIII. RECONSTRUCTION FROM UNIVARIATE TIME SERIES

Until now we have assumed that the starting point for our reconstruction was an ensemble of short trajectories in phase space, from which we reconstruct a long one by applying the DRTs algorithm. In many realistic situations we often can measure just one variable of the system under study. In such cases, if we can reconstruct the short phase space trajectories from each one of the univariate segments, then the process of generating a DRT is straightforward. Therefore, the question now is how to find the appropriate embedding parameters [24] from the ensemble of short univariate time series to first generate short phase space trajectories.

In order to estimate the embedding parameters, we use the following procedure: first, we concatenate the set of K short time series, each of length N and then, apply the usual methods for the estimation of the time delay and embedding dimension to the concatenated time series. To estimate the time delay τ , we apply two different techniques (i) first zero crossing of the autocorrelation function and (ii) the first minimum of the mutual information. It is important to stress here that both autocorrelation function and the mutual information of the concatenated time series are of course different from those of the underlying system. But the “jumps” in the envelope of both functions start at about a lag $\tau \geq N$. Hence, if the first zero crossing of the autocorrelation function or the first minima of the mutual information occur before N , then one can determine the embedding lag rather precisely. To estimate the embedding dimension m , we compute $2D_2$, where D_2 denotes the correlation dimension [29]. Since the correlation integral is a purely geometrical measure, it is not affected by the “jumps” in the trajectory as long as all the considered points are in the attractor [30,31].

We first exemplify the validity of this procedure, by considering the Rössler oscillator and estimating the embedding parameters for different ensembles generated by fixing K and varying N systematically. The obtained embedding delay τ and dimension m are compared to the ones estimated from a long univariate time series of length NK . For this, we consider an ensemble of $K=500$ short univariate time series by considering the x component of the Rössler system [Eq. (3)]. We vary N between 10 and 500 and estimate the embedding

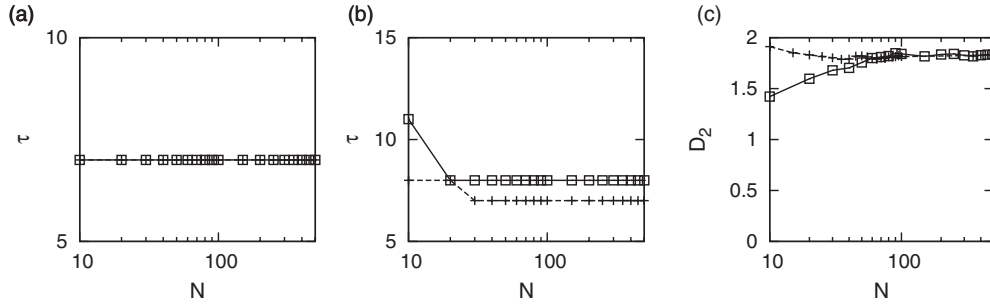


FIG. 10. Estimation of embedding parameters from an ensemble of short univariate time series in the case of the Rössler oscillator. (a) Estimated embedding delay (τ) by means of the autocorrelation function for the concatenated (squares) and for the original time series of length NK (plus signs) as a function of N . (b) The same as in (a), but by means of the mutual information. (c) Estimated correlation dimension (D_2) in dependence of N for the concatenated short trajectories (squares) and for the original time series of length NK (plus signs).

parameters τ and m for each value of N for both the concatenated time series (squares), and the original one (plus signs). As it can be clearly seen from Figs. 10(a) and 10(b), both the methods employed for the estimation of τ give a good estimate of τ for $N \geq 30$. Nevertheless, the autocorrelation function [Fig. 10(a)] performs better in this case, since it gives the correct estimate of τ (the same as the one given by the long original time series) already for $N=10$.

Figure 10(c) shows the estimated D_2 in dependence of N for both the concatenated time series (squares) and the original time series (plus-signs). These estimates of D_2 are obtained using Grassberger-Proccacia (GP) algorithm. The estimated D_2 for all the ensembles is $1.4 \leq D_2 \leq 2$ [32–35]. Hence, an appropriate choice for the embedding dimension is $m=4$. If we now embed each of the univariate short trajectories with the estimated embedding parameters $m=4$ and $\tau=7$, and then apply the DRT algorithm, we see that we can reproduce the dynamics of the underlying system rather well. Figure 11 shows a DRT generated from an ensemble of short univariate time series ($N=50, K=500$) of the Rössler oscillator for the parameters $p=0.02$ and $\xi=0.3$, after following the above embedding procedure. Since the DRT is constructed from just one of the components (x component) of the Rössler, the phase space projection is distorted. But the reconstructed phase space is topologically equivalent to that of the original attractor.

IX. EFFECT OF OBSERVATIONAL NOISE

It is crucial to analyse the robustness of the algorithm with respect to noisy short trajectories in order to study the applicability of the algorithm to real world data. Here, we consider the impact of observational noise on the DRTs. First, we add Gaussian white noise with standard deviation $S_{\text{noise}} = \sigma S_j$ to each component j of the short trajectories, where S_j is the standard deviation of the component j of the concatenated time series and σ is the noise level. Then we address the following question: does a DRT generated from noisy short trajectories (contaminated with a noise level of σ) resemble a LT, which is also contaminated with the same level of noise?

We again consider a collection of 5000 short trajectories from the Rössler system with 50 data points each. Our stud-

ies from the above sections show that rather good results are obtained for $p=0.03$ and $\xi=0.3$. Hence, we choose these parameters and generate DRTs from noise corrupted short trajectories and compare them to LTs corrupted by the same level of noise. Figure 12 shows the errors with respect to the autocorrelation function, mutual information and mean diagonal line in dependence of the level of noise. The error E_C in the autocorrelation function [Eq. (4)] does not show any particular response to the increasing level of noise; the error remains very small even for the highest levels of noise considered. On the other hand, the errors in the mutual information E_M [Eq. (4)] and in the mean diagonal line $E_{\bar{D}}$ [Eq. (5)] show a slightly increasing trend with higher levels of noise, but even then, the magnitude of the errors remains very small.

For levels of noise $\sigma > 9.0\%$ and the chosen parameters N, K, p , and ξ , the algorithm cannot generate a DRT, because

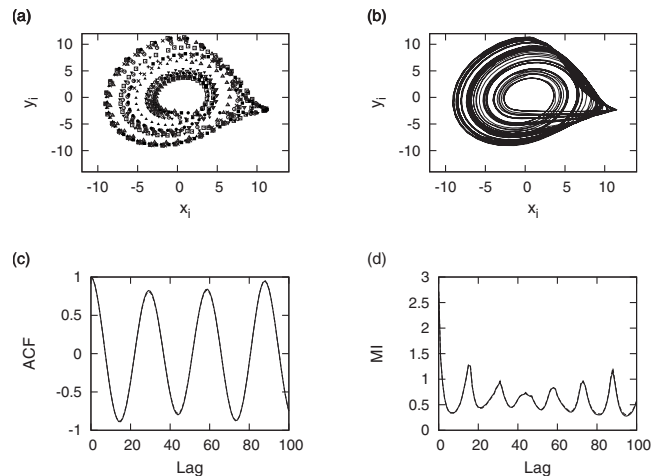


FIG. 11. DRT constructed from an ensemble of short univariate time series in the case of the Rössler oscillator. (a) Phase space projection of the embedded and concatenated univariate short trajectories. $N=50, K=500$. The different short trajectory types of the ensemble are plotted with different point types. (b) DRTs generated with the parameters $p=0.03$ and $\xi=0.3$. (c) Autocorrelation function for the DRT (solid line) and of an original LT (dashed line). (d) Mutual information function for the DRT (solid line) and for an original LT (dashed line). Notice that they are almost identical and hence, it is difficult to see the dashed line.

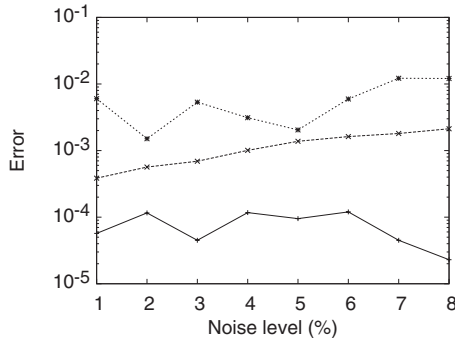


FIG. 12. Influence of observational noise on the quality of the DRTs generated from short trajectories of the Rössler system. The bold line is the error E_C in the autocorrelation function, the dashed line is the error E_M in the mutual information, and the dotted line is the error $E_{\bar{D}}$ in the mean diagonal line.

due to the noise, it does not find enough neighbors to which the trajectory can jump during the reconstruction. But this problem can be easily overcome, e. g., by increasing the number K of short trajectories. In the case that K is fixed by the experimental conditions, this problem can be solved by increasing the value of the threshold ξ . To monitor the errors made due to the increment of ξ , one can then consider Fig. 4 or 5.

X. APPLICATION TO ELECTROCHEMICAL DATA

The next challenge is to apply the algorithm to experimental situations where otherwise it is not possible to obtain long data sets that are necessary to understand the dynamics of the underlying systems. For example, assimilating long data sets from tracer particle trajectories and molecular dynamics experiments [36] is often not possible. Hence, our algorithm might play a key role in understanding the dynamics of a wide range of systems which have been so far not easy to handle.

It is therefore important to demonstrate first the validity of our algorithm with an experimental data. In this section we apply it to a scalar time series from an electrochemical experiment. The experimental setup consists of a nickel electrode immersed in sulfuric acid. The current at the electrode, measured at a constant applied potential, is directly proportional to the rate of metal dissolution. The measured current displays chaotic dynamics [37–39]. To justify the reconstruction algorithm with this experimental data, we first generate an artificial ensemble by randomly segmenting the measured univariate data and then generate a DRT by applying the reconstruction algorithm. We then compare the dynamics of the generated DRT to that of the embedded original scalar time series.

The original long time series consists of 33 026 data points and was measured at a rate of 2 kHz. This time series is cut at random points to generate an ensemble of nonoverlapping short segments. By leaving a random number of data points between two consecutive segments, we reproduce the practical problem of information loss in the artificially generated ensemble of short segments [Fig. 13(a)]. We generate

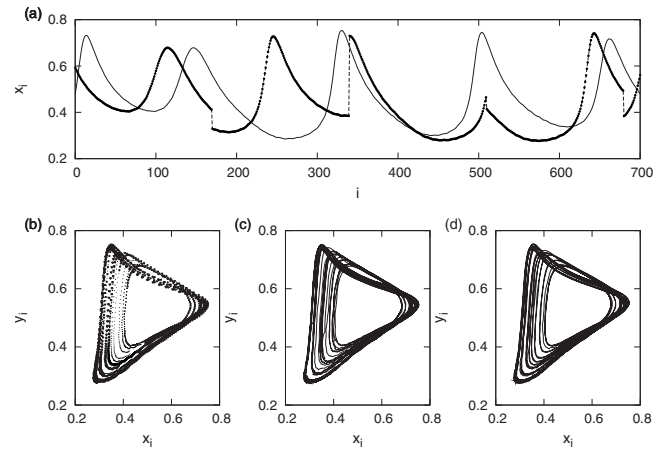


FIG. 13. (a) A segment of the original long time series (thin line) and the artificially generated concatenated time series (dotted line). Phase space projections of (b) the ensemble of embedded short trajectories, (c) generated DRTs, and (d) the original long time series after embedding.

an ensemble with $K=150$ segments, each consisting of $N=170$ data points (note that $NK < 33\,026$) [Fig. 13(b)]. As the next step, the embedding parameters are estimated from the concatenated univariate time series as described in Sec. VIII with the help of autocorrelation function and correlation dimension estimates. The embedding delay estimated from the autocorrelation function is found to be 26 and the correlation dimension estimate of the concatenated time series is $D_2=1.68$. Hence the estimated embedding dimension is 4. Each univariate short trajectory is then embedded, and the DRTs algorithm is applied to the ensemble of embedded short trajectories. The reconstructed DRT for a threshold of $\xi=0.012$ and $p=0.01$ is shown in Fig. 13(c).

On the other hand, the phase space of the original long scalar time series is reconstructed using standard embedding methods. The embedding delay is estimated from the autocorrelation function is also found to be 26. Next, we estimate the embedding dimension using the false nearest-neighbor method [24]. The embedding dimension is found to be 4. Note that both embedding parameters are the same as those obtained from the concatenated time series. The phase space of the original time series is shown in Fig. 13(d). It is clearly seen that the generated DRT resembles the phase space dynamics of the original long trajectory. Furthermore, the autocorrelation function and the mutual information of the original long time series is well reproduced by the generated DRT (Fig. 14).

XI. CONCLUSIONS

Short data sets render the application of many standard time series analysis techniques impossible. Different techniques, such as symbolic dynamics [40–42], order pattern recurrence plots [1] or wavelets [43,44], are often applied for the analysis of short data sets. However, depending on how short the time series are, the methods mentioned above are not applicable anymore. In this paper we have approached the problem from a different angle. We have proposed a new

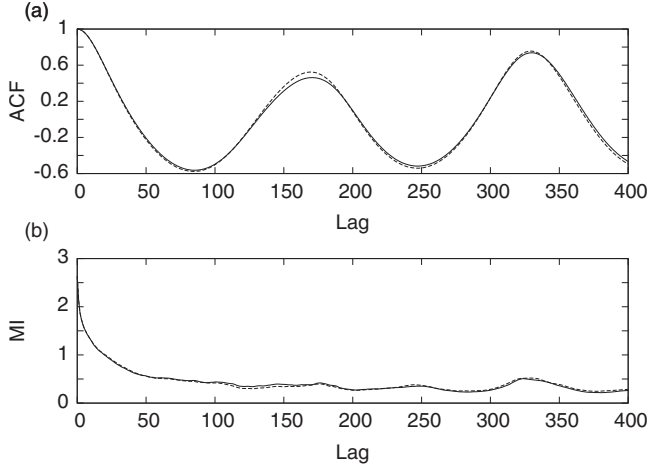


FIG. 14. Comparison of (a) the autocorrelation function and (b) the mutual information function of the generated DRTs (solid line) and original long (embedded) time series (dashed line).

algorithm which is capable of reconstructing a long trajectory (dynamically reconstructed trajectories, DRTs) of a system given an ensemble of short trajectories. This method uses the concept of recurrence in phase space. We have demonstrated that the DRTs very closely mimic the dynamics of the underlying system and reproduce its linear and nonlinear properties.

Moreover, we have studied the influence of the parameters ξ and p of the algorithm on the quality of the generated DRTs compared to an ensemble of original long trajectories (LTs). Furthermore, we have analyzed the dependence of the quality of the DRTs on the given number K and length N of the short trajectories. We have also addressed the important problem of reconstructing a long trajectory from univariate short time series.

The analysis of observational noise effects suggests that the algorithm is also quite efficient even if the short trajectories are corrupted by noise. Moreover, we have applied the algorithm to experimental data from electrochemical oscillators and shown that even in the case of real world data we can reproduce the dynamics of the original long trajectory accurately. This shows the potential of DRTs for the analysis of not only simulation data but also for experimental time series. A next step in this direction will be to apply the algorithm to further challenging sets of experimental data.

ACKNOWLEDGMENTS

The authors would like to thank John L. Hudson and Ist-

wan Z. Kiss for providing experimental data and proofreading the manuscript. C. K. thanks the Virtual Institute-Pole Equator Pole (PEP) and NATO projects for their financial support. M. C. R would like to acknowledge the Scottish Universities Life Science Alliance (SULSA) for the financial support. M. T would like to acknowledge the RUCK grant from EPSRC. N. M. was supported by Project No. MAP AO-2004-125 of the Microgravity Application Program/Biotechnology from the Human Spaceflight Program of the European Space Agency (ESA). J. K. would like to thank SFB 555 for the financial support.

APPENDIX: MEAN DIAGONAL LINE LENGTH FROM RP

Suppose that \vec{x}_i , with $i=1, \dots, L$, is a trajectory in a d -dimensional phase space. Then, the recurrence matrix is defined as

$$R_{i,j} = \Theta(\varepsilon - \|\vec{x}_i - \vec{x}_j\|), \quad i, j = 1, \dots, L, \quad (A1)$$

where ε is a predefined threshold, $\Theta(\cdot)$ is the Heaviside step function and $\|\cdot\|$ is a norm, e.g., the Euclidean or the maximum norm. The graphical representation of the recurrence matrix, obtained by encoding the ones by black and zeros by white dots, is called recurrence plot (RP). Figure 15 shows the RPs of some prototypical systems. A periodic trajectory in phase space (e.g., a circle in the phase space) can be represented by a two-dimensional system of equations $x_i = \sin(2\pi i/100)$, $y_i = \cos(2\pi i/100)$. The RP of such a system is characterized by noninterrupted continuous diagonal lines, whereas the RP of white noise consists of mainly single points. The RP of the Rössler system in the chaotic regime consists of interrupted diagonal lines.

As Fig. 15 illustrates, the length and the distribution of the diagonal lines in an RP is related to main properties of the underlying systems. Longer comoving segments of the phase space are represented by longer diagonal lines of an RP and shorter comoving segments correspond to short diagonal lines. In fact, it has been reported in Ref. [9] that the cumulative distribution of the diagonal lines is related to the second order Rényi entropy (K_2) [24]. K_2 quantifies how rapidly the number of possible future evolutions increases with time. For periodic systems $K_2=0$, for stochastic systems $K_2 \rightarrow \infty$ and for chaotic systems K_2 takes a finite, positive value. K_2 can be estimated from the cumulative distribution of diagonal lines in an RP by

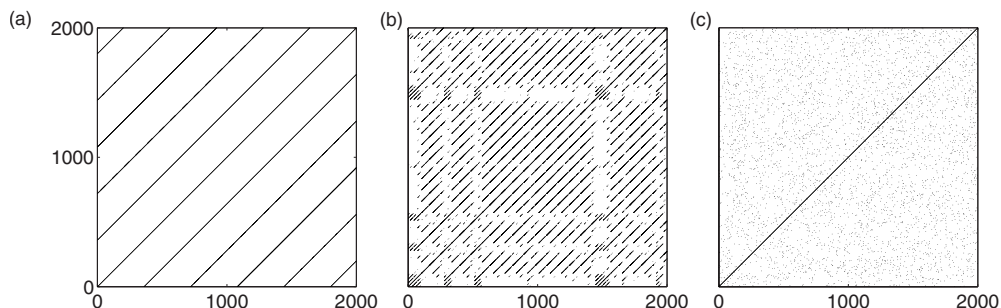


FIG. 15. RPs of (a) a periodic trajectory in phase space, (b) the Rössler oscillator in the chaotic regime, and (c) white noise.

$$P_\varepsilon^c(l) \sim \varepsilon^{D_2} \exp[-K_2(\varepsilon)\Delta t l], \quad (\text{A2})$$

where $P_\varepsilon^c(l)$ is the cumulative distribution of diagonal lines in the RP, i.e., the probability of finding a diagonal line of at least length l . D_2 is the correlation dimension of the system under consideration and Δt is the sampling rate of the time series. If we plot $P_\varepsilon^c(l)$ in a logarithmic scale versus l , we obtain a straight line with slope $-K_2(\varepsilon)\Delta t$ for large l . Hence, the mean diagonal line \bar{D}

$$\bar{D} = \frac{\sum_{l=2}^N l P(l)}{\sum_{l=1}^N l P(l)} \quad (\text{A3})$$

of an RP is an estimate for K_2 [1]. $P(l)$ in Eq. (A3) denotes the probability to find a diagonal line of length l in an RP. Moreover, \bar{D} is numerically straightforward and fast to compute.

-
- [1] N. Marwan, M. C. Romano, M. Thiel, and J. Kurths, *Phys. Rep.* **438**, 237 (2007).
- [2] H. Poincaré, *Acta Math.* **13**, 1 (1890).
- [3] J. P. Eckmann, S. O. Kamphorst, and D. Rulle, *Europhys. Lett.* **4**, 973 (1987).
- [4] J. P. Zbilut and C. L. Webber, Jr., *Phys. Lett. A* **171**, 199 (1992).
- [5] N. Marwan, N. Wessel, U. Meyerfeldt, A. Schirdewan, and J. Kurths, *Phys. Rev. E* **66**, 026702 (2002).
- [6] C. Letellier, *Phys. Rev. Lett.* **96**, 254102 (2006).
- [7] E. J. Nagamga, A. Nandi, R. Ramaswamy, M. C. Romano, M. Thiel, and J. Kurths, *Phys. Rev. E* **75**, 036222 (2007).
- [8] M. C. Romano, M. Thiel, J. Kurths, I. Z. Kiss, and J. Hudson, *Europhys. Lett.* **71**, 466 (2005).
- [9] M. Thiel, M. C. Romano, P. L. Read, and J. Kurths, *Chaos* **14**, 234 (2004).
- [10] M. Thiel, M. C. Romano, and J. Kurths, *Phys. Lett. A* **330**, 343 (2004).
- [11] M. Thiel, M. C. Romano, J. Kurths, M. Rolf, and R. Kliegl, *Europhys. Lett.* **75**, 535 (2006).
- [12] A. Giuliani and C. Manetti, *Phys. Rev. E* **53**, 6336 (1996).
- [13] A. S. Elwakil and A. M. Soliman, *Chaos, Solitons Fractals* **10**, 1399 (1999).
- [14] J. M. Nicholas, S. T. Trickey, and M. Seaver, *Mech. Syst. Signal Process.* **20**, 421 (2006).
- [15] N. Marwan, M. Thiel, and N. R. Nowaczyk, *Nonlinear Processes Geophys.* **9**, 325 (2002).
- [16] N. Marwan, M. H. Trauth, M. Vuille, and J. Kurths, *Clim. Dyn.* **21**, 317 (2003).
- [17] T. K. March, S. C. Chapman, and R. O. Dendy, *Physica D* **200**, 171 (2005).
- [18] J. Kurths, U. Schwarz, C. P. Sonett, and U. Parlitz, *Nonlinear Processes Geophys.* **1**, 72 (1994).
- [19] N. Asghari, C. Broeg, L. Carone, R. Casas-Miranda, J. C. Castro Palacio, I. Csillik, R. Dvorak, F. Freistetter, G. Hadjivan-tsides, H. Hussmann, A. Khranova, M. Khristoforova, I. Khromova, I. Kitiashvilli, S. Kozłowski, T. Laakso, T. Lacz-kowski, D. Lytvinenko, O. Miloni, R. Morishima, A. Moro-Martin, V. Paksyutov, A. Pal, V. Patidar, B. Pecnik, O. Peles, J. Pyo, T. Quinn, A. Rodriguez, C. Romano, E. Saikia, J. Stadel, M. Thiel, N. Todorovic, D. Veras, E. Vieira Neto, J. Vilagi, W. von Bloh, R. Zechner, and E. Zhuchkova, *Astron. Astrophys.* **426**, 353 (2004).
- [20] N. V. Zolotova and D. I. Ponyavin, *Astron. Astrophys.* **449**, L1 (2006).
- [21] I. M. János and T. Tél, *Phys. Rev. E* **49**, 2756 (1994).
- [22] We refer to the future of \vec{x}_i as \vec{x}_{i+1} .
- [23] Note that \vec{x}_m is considered to be a neighbor of itself, i.e., it is also possible to jump to its own future.
- [24] H. Kantz and T. Schreiber, *Nonlinear Time Series Analysis*, 2nd ed. (Cambridge University Press, Cambridge, 2004).
- [25] M. Hénon, *Commun. Math. Phys.* **50**, 69 (1976).
- [26] R. P.-Satorras and R. H. Riedi, *J. Phys. A* **29**, L391 (1996).
- [27] P. Grassberger and I. Procaccia, *Physica D* **13**, 34 (1984).
- [28] O. E. Rossler, *Phys. Lett. A* **71**, 155 (1979).
- [29] P. Grassberger and I. Procaccia, *Phys. Rev. Lett.* **50**, 346 (1983).
- [30] M. Dhamala, Y.-C. Lai, and E. J. Kostelisch, *Phys. Rev. E* **64**, 056207 (2001).
- [31] M. Dhamala, G. Pagnoni, K. Wiesenfeld, and G. S. Berns, *Phys. Rev. E* **65**, 041917 (2002).
- [32] M. Ding, C. Grebogi, E. Ott, T. Sauer, and J. A. Yorke, *Phys. Rev. Lett.* **70**, 3872 (1993).
- [33] C. Raab and J. Kurths, *Phys. Rev. E* **64**, 016216 (2001).
- [34] J. C. Sprott, *Int. J. Bifurcation Chaos Appl. Sci. Eng.* **11**, 1865 (2001).
- [35] Due to the effects of finite data sets (for lower values of N), boundary problems and slower convergence of the correlation integral in the case of systems like Rössler which has nonuniform measure, the estimates of D_2 when computed using GP algorithm, are usually less than the theoretical value of 2 ± 0.05 .
- [36] J. D. Chodera, W. C. Swope, J. W. Pitera, and K. A. Dill, *Multiscale Model. Simul.* **5**, 1214 (2006).
- [37] I. Z. Kiss and J. L. Hudson, *Phys. Chem. Chem. Phys.* **4**, 2638 (2002).
- [38] I. Z. Kiss and J. L. Hudson, *Phys. Rev. E* **64**, 046215 (2001).
- [39] I. Z. Kiss, W. Wang, and J. L. Hudson, *Phys. Chem. Chem. Phys.* **2**, 3847 (2000).
- [40] D. Lind and B. Marcus, *An Introduction to Symbolic Dynamics and Coding* (Cambridge University Press, Cambridge, 1995).
- [41] P. B. Graben, J. D. Saddy, M. Schlesewsky, and J. Kurths, *Phys. Rev. E* **62**, 5518 (2000).
- [42] N. Wessel, C. Ziehm, J. Kurths, U. Meyerfeldt, A. Schirdewan, and A. Voss, *Phys. Rev. E* **61**, 733 (2000).
- [43] S. Mallet, *A Wavelet Tour of Signal Processing* (Academic Press, San Diego, 1998).
- [44] J. J. Chao and C. C. Lin, *1997 International Conference on Image Processing (ICIP'97)* (IEEE, Los Alamitos, CA, 1997), Vol. 2, pp. 354–357.